Electronic Supplementary Material (ESI) for ChemComm.

Electronic Supplementary Information

Supramolecular polymerization of thiobarbituric acid naphthalene dye

Takumi Aizawa [a], Maika Kawaura,[a] Takashi Kajitani[b], Kowit Hengphasatporn[c], Yasuteru Shigeta[c]*
Shiki Yagai*[d,f]

[a] *Division of Advanced Science and Engineering, Graduate School of Engineering, Chiba University, 1-33 Yayoi-cho, Inage-ku, Chiba 263-8522, Japan.*

[b] *Open Facility development office, Open Facility Center, Tokyo Institute of Technology, 4259 Nagatsuta, Midori-ku, Yokohama 226-8503, Japan.*

[c] *Center for Computational Sciences, University of Tsukuba, 1-1-1 Tennodai, Tsukuba, Ibaraki 305-8577, Japan.*

[d] *Department of Applied Chemistry and Biotechnology, Graduate School of Engineering, Chiba University, 1-33 Yayoi-cho, Inage-ku, Chiba 263-8522, Japan.*

[e] *Institute for Advanced Academic Research (IAAR), Chiba University, 1-33, Yayoi-cho, Inage-ku, Chiba 263-8522, Japan.*

E-mail: yagai@faculty.chiba-u.jp

Table of Contents

1. Material and Methods

General: All commercially available reagents and solvents were of reagent grade and used without further purification. The solvents for the preparation of the assemblies were all spectral grade and used without further purification. ^{1}H and ^{13}C NMR spectra were recorded on a JEOL JNM-ECA500 NMR spectrometer and chemical shifts are reported in ppm (δ) with the signal of TMS as the internal standard. APCI-MS spectra were measured on an Exactive (Thermo Scientific). UV–vis spectra were recorded on a JASCO V660 spectrophotometer equipped with a Peltier device temperature-control unit. FT-IR spectra were measured on a JASCO FT/IR-4600 spectrometer. AFM images were acquired under ambient conditions using Multimode 8 Nanoscope V (Bruker Instruments) in Peak Force Tapping (Scanasyst) mode. Silicon cantilevers (SCANASYST-AIR) with a spring constant of 0.4 N/m and frequency of 70 kHz (nominal value, Bruker, Japan) were used. The samples were prepared by spin-coating MCH solutions (10 μL) onto freshly cleaved highly-oriented pyrolytic graphite (HOPG) at 3000 rpm for 1 min.

Powder X-ray diffraction analysis: Powder XRD patterns of the bulk sample were measured using 0.154 nm X-ray (CuKα-beam) in the transparent mode using NANO-Viewer (Rigaku Corp.) equipped with a Pilatus 100K (Dectris) detector. The scattering angle (2θ) and the position of the incident X-ray beam on the detectors were calibrated using several orders of layer reflections from silver behenate (d = 58.380 Å). The sample-to-detector distance was 7 cm. The obtained diffraction patterns were integrated along the Debye–Scherrer ring to afford 1D intensity data using 2DP software (Rigaku Corp.).

Small-angle X-ray scattering (SAXS): SAXS measurements were carried out at BL-10C at the Photon Factory of the High Energy Accelerator Research Organization (KEK) in Tsukuba, Japan. Solutions were loaded into cells (stainless steel surround, 20-μm-thick quartz glass windows, 1.25-mm-path length), and the temperature was maintained at around 293 K (room temperature). X-ray wavelength of 1.5 Å and a sample-detector distance of 1029 mm (calibrated using silver behenate) gave a detectable Q range of the order of 0.1 to 5.9 nm^{-1}. Sixty frames were collected with an exposure time of 10 s: Radiation damage was not observed, so these data were averaged to give a total integration time of 600 s. The 2D scattering data (detector: DECTRIS PILATUS3 2M) were radially averaged to yield 1D scattering intensity data [$I(Q)$ versus Q]. This was normalized using water as a reference, and the solvent + cell background was subtracted, to give absolute scattering intensity $I(Q)$ in cm^{-1}.

Quantum Chemical Calculations: Optimized structures of the hydrogen-bonding dimers and cyclic hexamers were performed with B3LYP-GD3BJ /6-31+G(d,p) level by using Gaussian 16 program package [1-8] on an in-house computer cluster. The results for the *syn* dimers and the cyclic hexamers are shown in Figs. S2 and S3, respectively. Since the angle between the vectors of two C=O bonds in the *syn* dimer of **1'** is close to 60 degree, the cyclic hexamer of **1'** has a planar structure. On the other hand, the cyclic hexamer of **2'** has a non-planar structure because the angle between the vectors of two C=S bonds in the *syn* dimer of **2'** is about 44 degree. To estimate vibrational frequencies of **1'** and **2'**, the vibrational analysis was performed for monomer by using the same calculation level. The obtained results are summarized in Fig. 3, S2 and S3, where GaussView 6 was used to depict the normal modes [9].

[1] A. D. Becke, *J. Chem. Phys.*, **98**, 5648 (1993).

[2] S. Grimme, S. Ehrlich and L. Goerigk, J. Comp. Chem., **32**, 1456 (2011).

[3] W. J. Hehre, R. Ditchfield, and J. A. Pople, *J. Chem. Phys.*, **56**, 2257(1972).

[4] P. C. Hariharan and J. A. Pople, *Theor. Chem. Acc.*, **28,** 213-22 (1973).

[5] M. M. Francl, W. J. Pietro, W. J. Hehre, J. S. Binkley, D. J. DeFrees, J. A. Pople, and M. S. Gordon, *J. Chem. Phys.*, **77**, 3654 (1982).

[6] T. Clark, J. Chandrasekhar, G. W. Spitznagel, and P. v. R. Schleyer, *J. Comp. Chem.* **4**, 294-301 (1983).

[7] M. J. Frisch, J. A. Pople, and J. S. Binkley, *J. Chem. Phys.*, **80**, 3265 (1984).

[8] Gaussian 16, Revision C.01, M. J. Frisch, G. W. Trucks, H. B. Schlegel, G. E. Scuseria, M. A. Robb, J. R. Cheeseman, G. Scalmani, V. Barone, G. A. Petersson, H. Nakatsuji, X. Li, M. Caricato, A. V. Marenich, J. Bloino, B. G. Janesko, R. Gomperts, B. Mennucci, H. P. Hratchian, J. V. Ortiz, A. F. Izmaylov, J. L. Sonnenberg, D. Williams-Young, F. Ding, F. Lipparini, F. Egidi, J. Goings, B. Peng, A. Petrone, T. Henderson, D. Ranasinghe, V. G. Zakrzewski, J. Gao, N. Rega, G. Zheng, W. Liang, M. Hada, M. Ehara, K. Toyota, R. Fukuda, J. Hasegawa, M. Ishida, T. Nakajima, Y. Honda, O. Kitao, H. Nakai, T. Vreven, K. Throssell, J. A. Montgomery, Jr., J. E. Peralta, F. Ogliaro, M. J. Bearpark, J. J. Heyd, E. N. Brothers, K. N. Kudin, V. N. Staroverov, T. A. Keith, R. Kobayashi, J. Normand, K. Raghavachari, A. P. Rendell, J. C. Burant, S. S. Iyengar, J. Tomasi, M. Cossi, J. M. Millam, M. Klene, C. Adamo, R. Cammi, J. W. Ochterski, R. L. Martin, K. Morokuma, O. Farkas, J. B. Foresman, and D. J. Fox, Gaussian, Inc., Wallingford CT, 2016.

[9] GaussView, Version 6.1, Roy Dennington, Todd A. Keith, and John M. Millam, Semichem Inc., Shawnee Mission, KS, 2016.

2. Synthesis and Analytical Datas

Synthesis of compounds **1** and **3** were reported previously. [10]

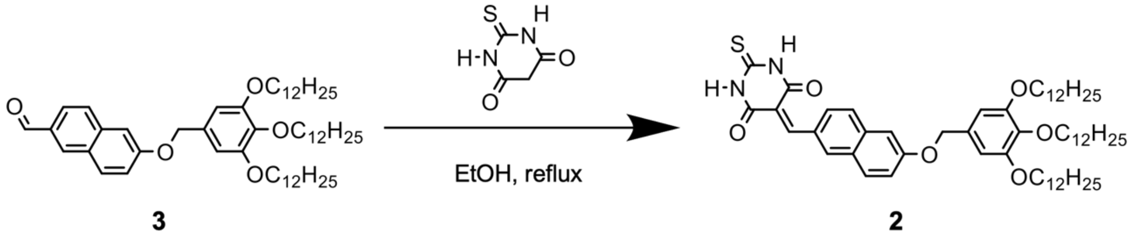

Scheme S1. Synthesis of compound **2**.

Synthesis of compound 2: Compound **3** (150 mg, 184 μmol) and 2-thiobarbituric acid (26 mg, 184 μmol) in EtOH (10 mL) was refluxed at 75 °C for 24 h. The reaction mixture was cooled to r.t. and the resulting precipitates were collected by filtration and washed with hot EtOH repeatedly. The residual solid was further purified by reprecipitation from a $CHCl_3$-MeOH mixture to give pure compound **1** as an orange solid (106 mg, 61 %). ^{1}H NMR (400 MHz, $CDCl_3$, 293K): δ= 9.16 (br, 1H), 9.13 (br, 1H), 8.84 (s, 1H), 8.72 (s, 1H), 8.37 (dd, J = 8.93 Hz, 1.59 Hz, 1H), 7.92 (d, J = 8.99 Hz, 1H), 7.76 (d, J = 8.93 Hz, 1H), 7.29 (dd, J = 8.99 Hz, 2.45 Hz, 1H), 7.23 (d, J = 4.28 Hz, 1H), 6.67 (s, 2H), 5.11 (s, 2H) 4.01–3.94 (m, 6H), 1.84–1.72 (m, 6H), 1.51–1.26 (m, 63H), 0.89–0.86 (m, 9H). ^{13}C NMR (400 MHz, $CDCl_3$, 333K): δ= 176.09, 161.65, 160.98, 153.53, 139.46, 138.93, 138.33, 132.27, 130.98, 130.85, 128.26, 126.96, 120.16, 114.52, 107.68, 106.87, 73.46, 70.75, 69.55, 69.44 31.84, 30.36, 29.76, 29.65, 29.61, 29.57, 29.52, 29.37, 29.25, 26.21, 26.09, 22.57 13.87. HRMS(APCI) *m/z* calcd for $C_{58}H_{89}O_6N_2S$ 941.6436 [M+H]+, found 941.6450.

[10] S. Yagai, Y. Goto, L. Xu, T. Karatsu, A. Kitamura, D. Kuzuhara, H. Yamada, Y. Kikkawa, A. Saeki, and S. Seki, *Angew. Chem. Int. Ed.*, 2012, **51**, 6643-6647.

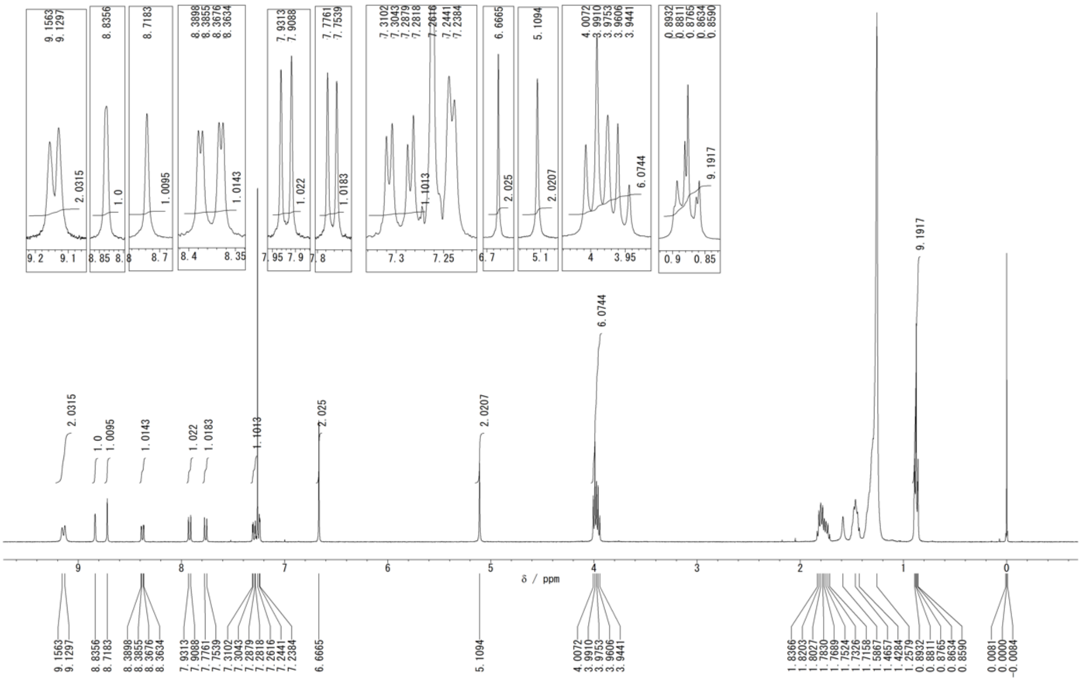

Chart S1. ^{1}H NMR spectrum of compound **2** in $CDCl_3$ at 293 K.

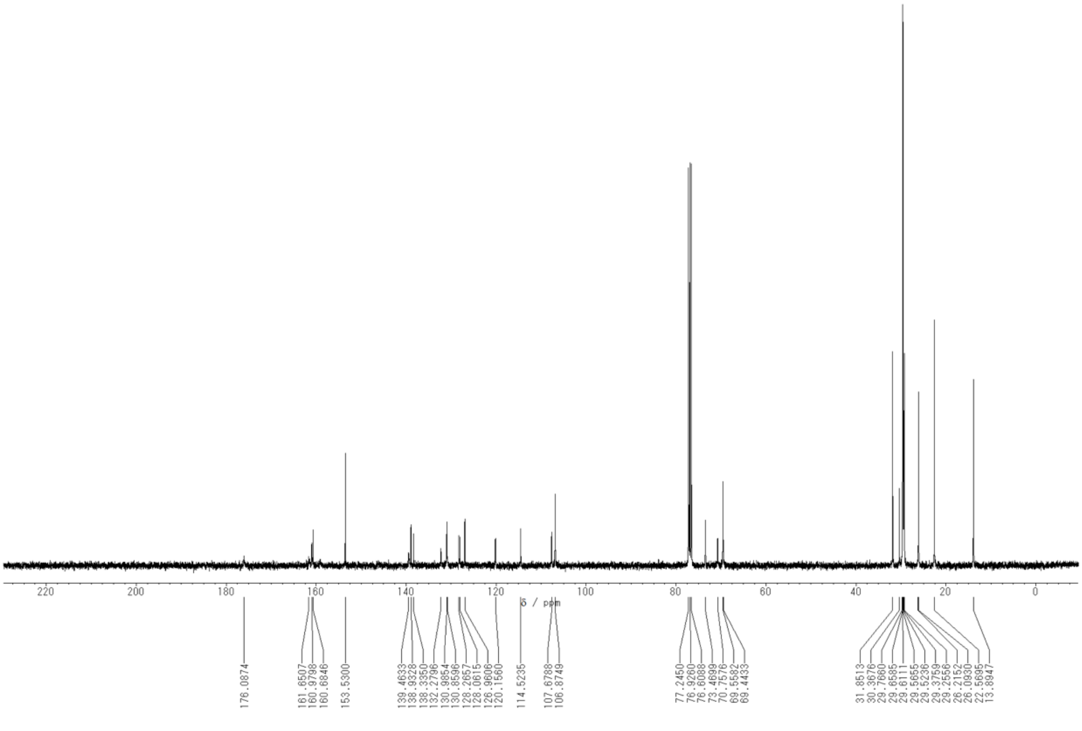

Chart S2. ^{13}C NMR spectrum of compound **2** in $CDCl_3$ at 333 K.

3. Supporting Figures

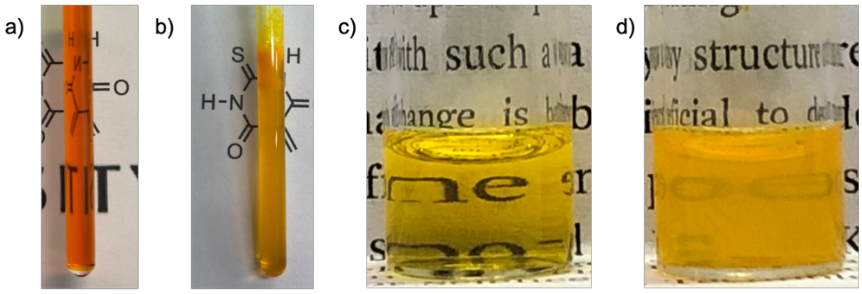

Fig. S1 (a,b) Photographs of $CHCl_3$ solutions of **1** at c = 100 mM (a) and **2** at c = 10 mM (b). (c,d) Photographs of MCH solutions of **1** at c = 0.5 mM (a), and **2** at c = 0.5 mM (b).

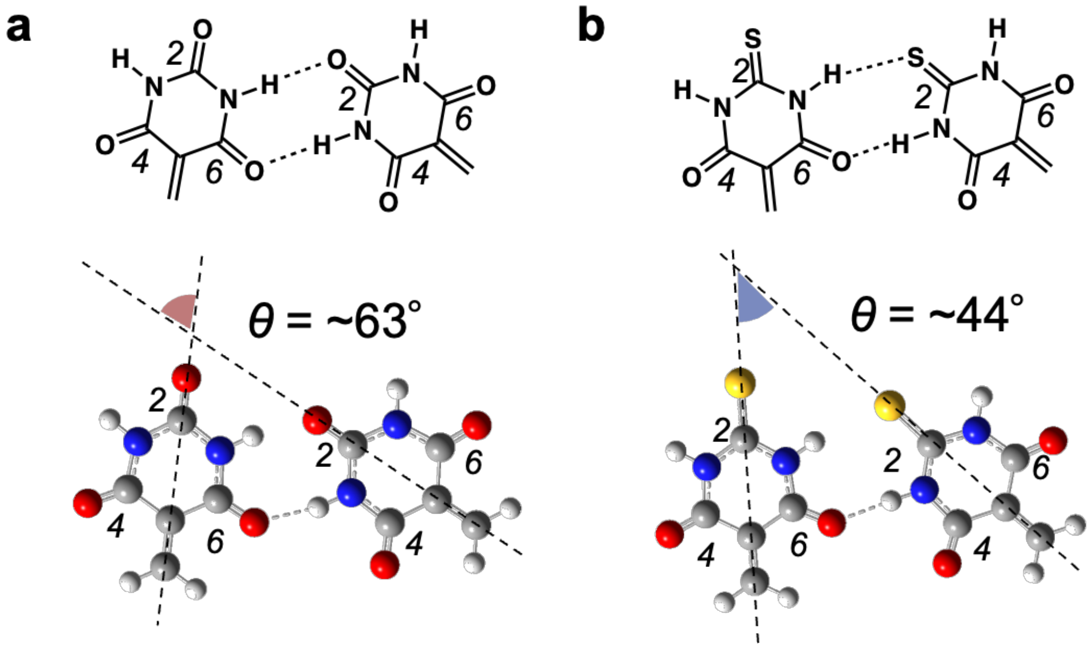

Fig. S2 Chemical structures (top) and DFT-optimized structures (bottom) of *syn* dimers of (a) model molecule **1'** [barbituric acid (5-(propan-2-ylidene)pyrimidine-2,4,6(1H,3H,5H)-trione)] and (b) **2'** [2-thiobarbituric acid (5-(propan-2-ylidene)-2-thioxodihydropyrimidine-4,6(1H,5H)-dione)].

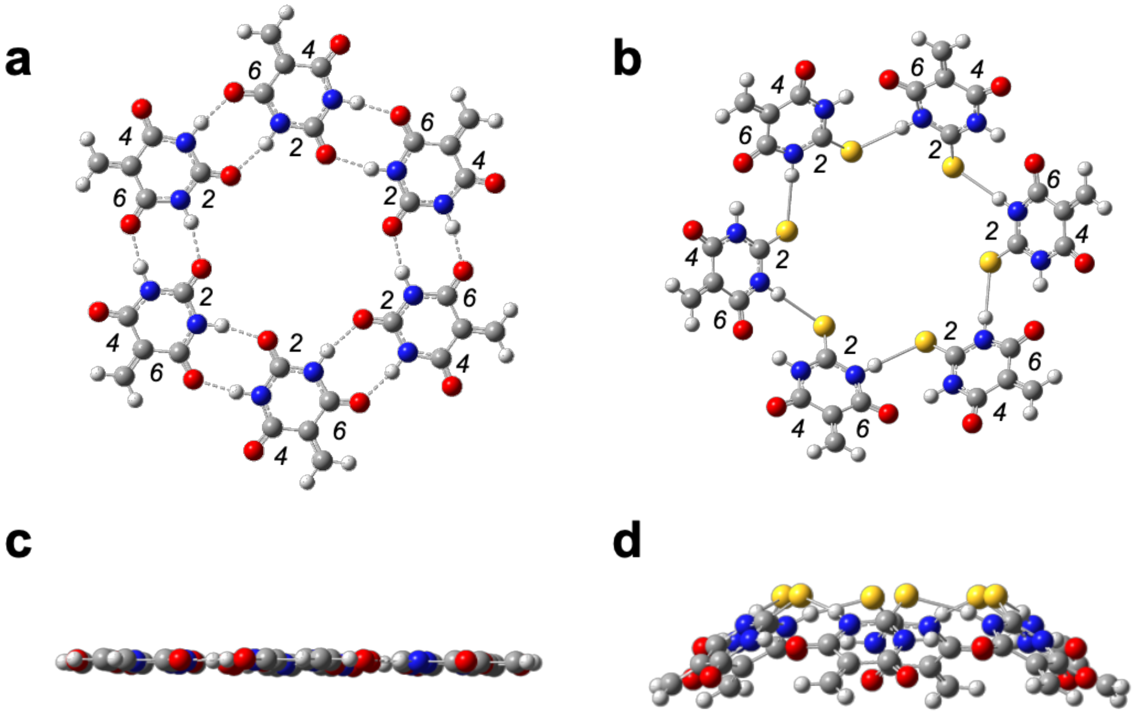

Fig. S3 Top (a,b) and side views (c,d) of cyclic hexamers of **1'** (a,c) and **2'** (b,d) optimized by DFT calculations.

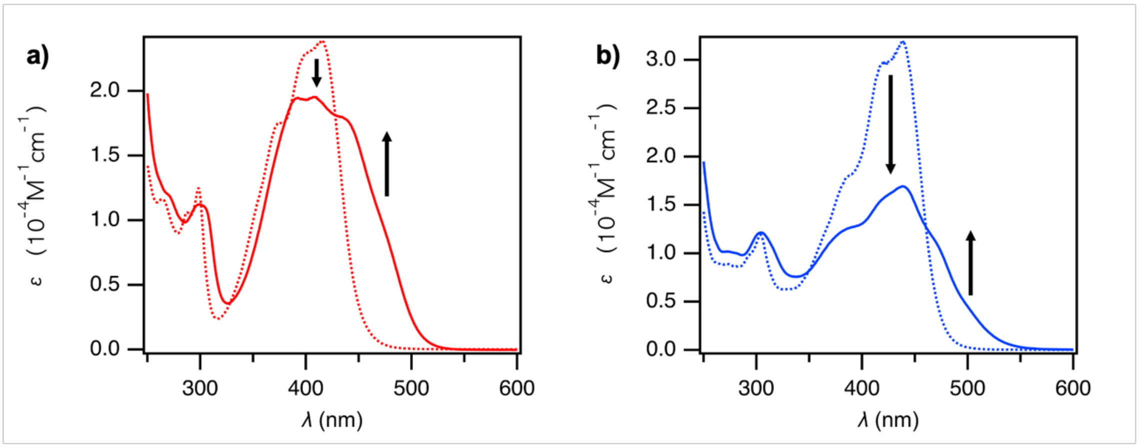

Fig. S4 UV-Vis spectra of **1** (a) and **2** (b) in MCH (c = 0.12 mM) at 100 °C (dotted lines) and 20 °C (solid lines) upon cooling at the rate of 1 °C min^{-1}.

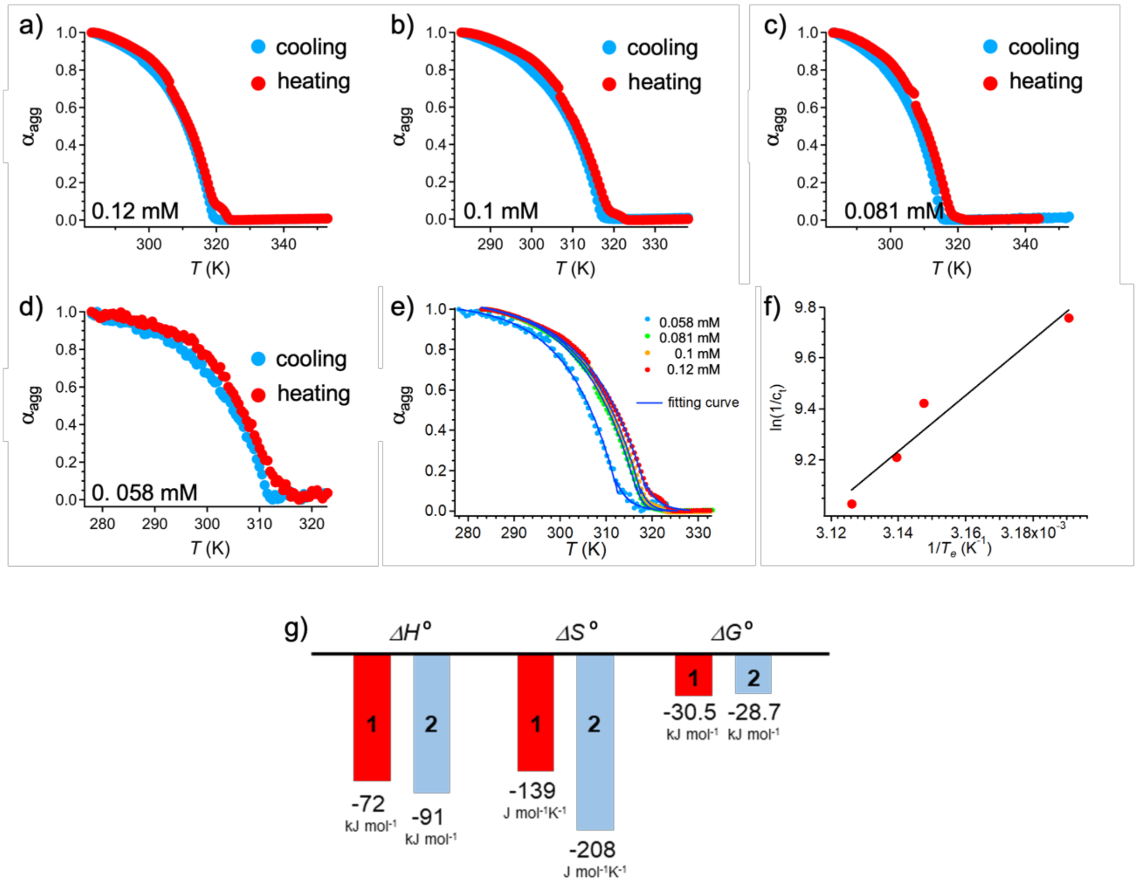

Fig. S5 (a-d) Degree of aggregation (α_{agg}) of **2** (a, 0.12 mM; b, 0.1 mM; c, 0.081 mM; d, 0.058 mM) as a function of temperature during cooling (blue dots) and heating (red dots) in MCH at a rate of 1 °Cmin^{-1}. α_{agg} was calculated from absorbance changes at 520 nm. (e) Fitting analysis of the heating curves with a cooperative supramolecular polymerization model developed by Meijer and co-workers[11]. (f) van't Hoff plot of the natural logarithm of the reciprocal concentration as a function of the reciprocal elongation temperature (1/T_e). The black line shows the corresponding linear fit. (g) Comparison of the thermodynamic parameters evaluated from the van't Hoff analysis. The data of **1** were quoted from a previous study.[12]

[11] (a) D. Zhao, J. S. Moore, *Org. Biomol. Chem.* 2003, **1**, 3471; (b) P. Jonkheijm, P. van der Schoot, A. P. H. J. Schenning, and E. W. Meijer, *Science* 2006, **313**, 80; (c) M. M. J. Smulders, M. M. L. Nieuwenhuizen, T. F. A. de Greef, P. van der Schoot, A. P. H. J. Schenning, and E. W. Meijer, *Chem.—Eur. J.* 2010, **16**, 362.

[12] K. Aratsu, R. Takeya, B. R. Pauw, M. J. Hollamby, Y. Kitamoto, N. Shimizu, H. Takagi, R. Haruki, S. Adachi, and S.Yagai, *Nature Commun*., 2020, **11**, Article number: 1623.

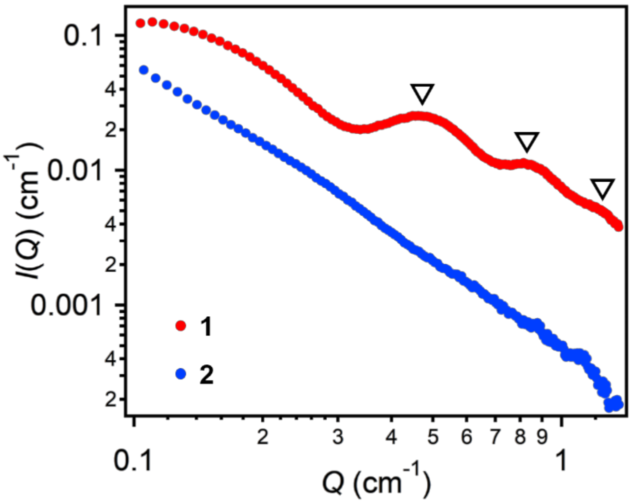

Figure. S6 SAXS profiles of **1** (red dots) and **2** (red dots) in MCH (c = 0.15 mM).

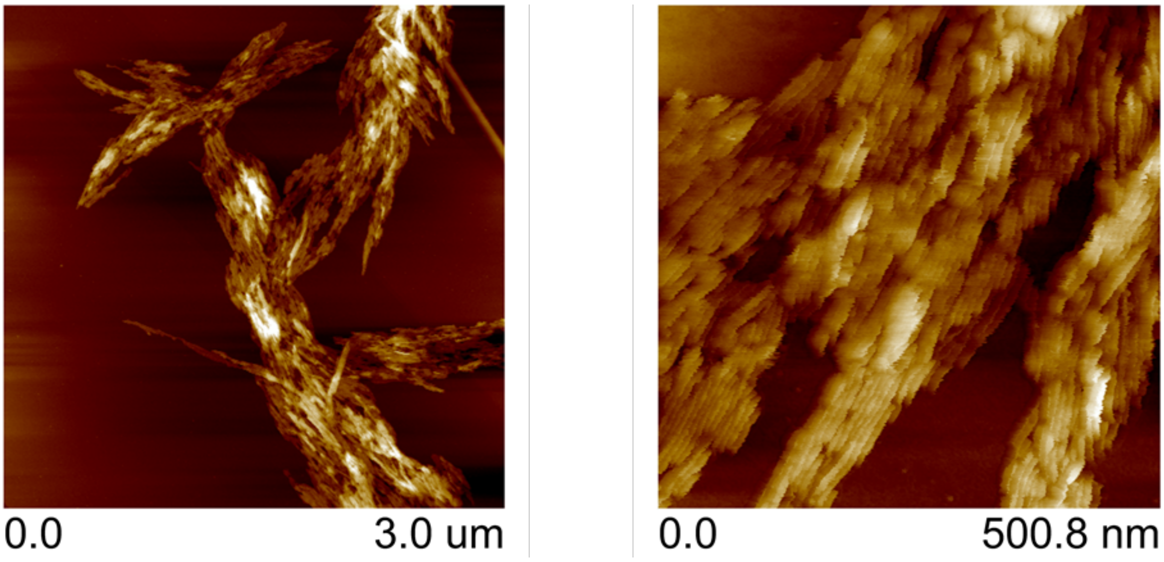

Figure. S7 Additional AFM images of aggregates of **2** formed in MCH (c = 0.5 mM) upon cooling from 100 ºC to 20 ºC.

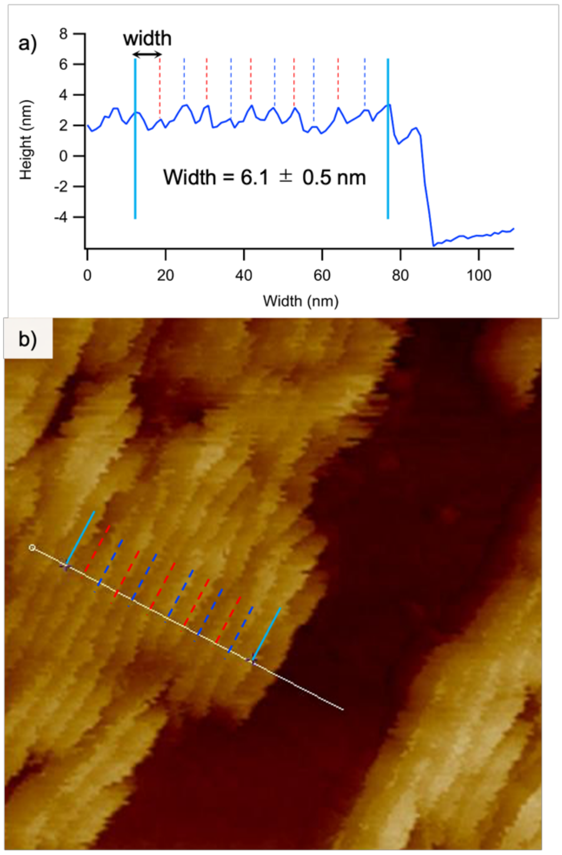

Figure. S8. (a) Cross-sectional analysis along the white lines in the image of (b).

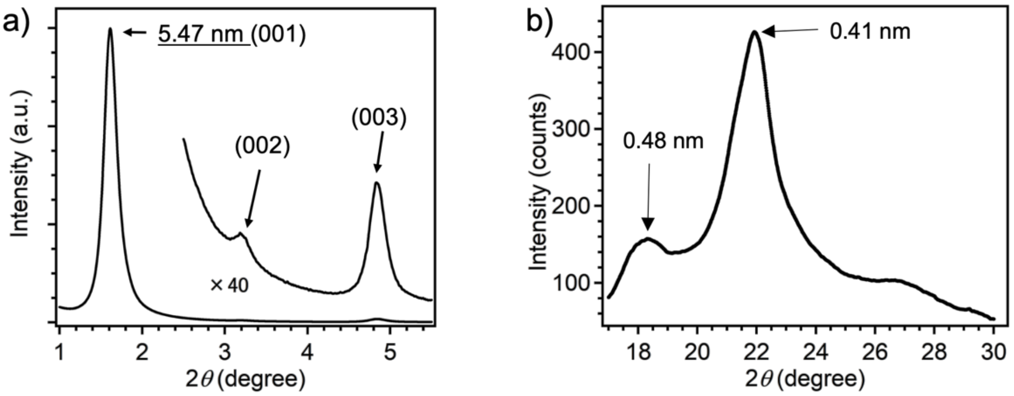

Fig. S9 (a,b) The powder XRD pattern of precipitates of **2**, which were obtained by aging the MCH solution (c = 0.5 mM) at room temperature. (a) Small-angle region and (b) Wide-angle region.

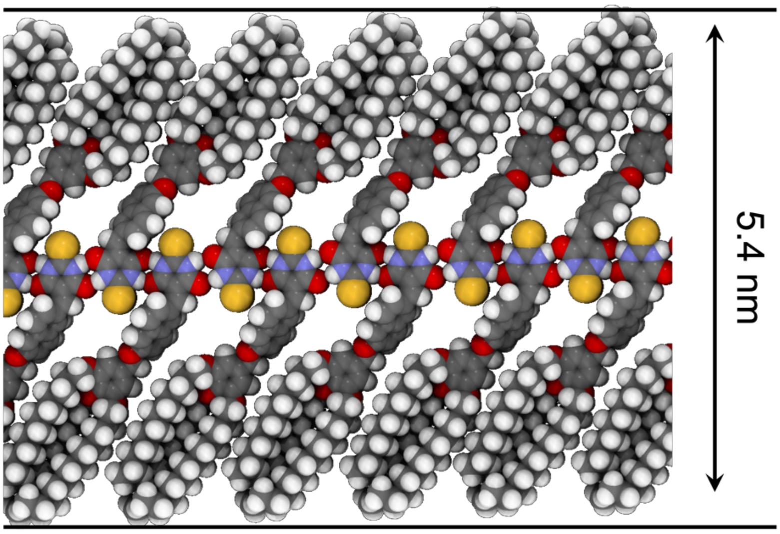

Fig. S10 A molecular modelled tape-like aggregate of **2** using hydrogen-bonding between NHC(4)=O and NHC(6)=O groups.

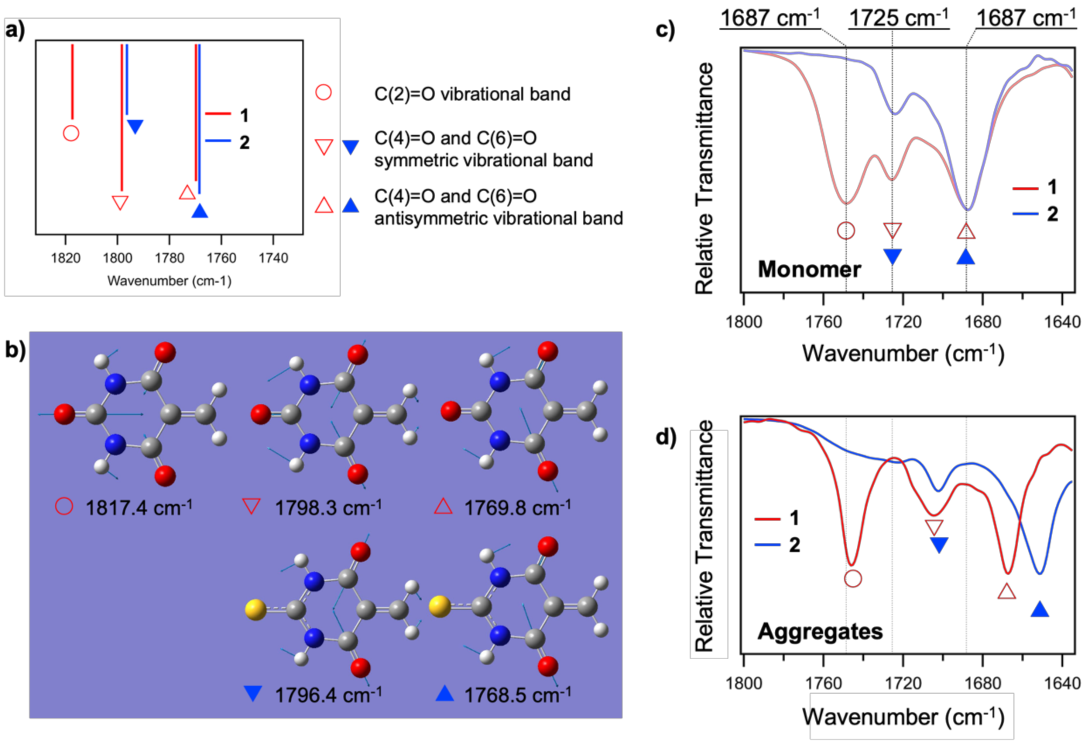

Fig. S11 (a) Calculated IR spectra of model molecules of **1’** [barbituric acid (5-(propan-2-ylidene)pyrimidine-2,4,6(1H,3H,5H)-trione)] and **2’** [2-thiobarbituric acid (5-(propan-2-ylidene)-2-thioxodihydropyrimidine-4,6(1H,5H)-dione)] by DFT (B3LYP+GD3BJ level) in the gas phase. (b)

Simulated vibrational modes of each wavenumber. (c,d) IR spectra of **1** (red line) and **2** (blue line) in $CHCl_3$ (c, *c* = 2 mM) and nanofiber film on KBr substrate (d). For these spectra of **1**, the peak marked with ○ can be assigned to the vibrational band of C(2)=O group. For spectra of **1** and **2**, peaks marked with ▽/▼ can be assigned to the symmetric vibrational band of C(4)=O and C(6)=O, and those marked with △/▲ can be assigned to antisymmetric vibrational band of C(4)=O and C(6)=O.